Analysis and Synthesis of Pseudo-Periodic 1/*f*-Like Noise by Means of Wavelets with Applications to Digital Audio

Pietro Polotti

Laboratoire de Communications Audiovisuelles (LCAV) École Polytechnique Fédérale de Lausanne, Switzerland
Email: pietro.polotti@epfl.ch

Gianpaolo Evangelista

Laboratoire de Communications Audiovisuelles (LCAV) École Polytechnique Fédérale de Lausanne, Switzerland
Email: gianpaolo.evangelista@epfl.ch

Voiced musical sounds have nonzero energy in sidebands of the frequency partials. Our work is based on the assumption, often experimentally verified, that the energy distribution of the sidebands is shaped as powers of the inverse of the distance from the closest partial. The power spectrum of these pseudo-periodic processes is modeled by means of a superposition of modulated $1/f$ components, that is, by a pseudo-periodic $1/f$-like process. Due to the fundamental selfsimilar character of the wavelet transform, $1/f$ processes can be fruitfully analyzed and synthesized by means of wavelets. We obtain a set of very loosely correlated coefficients at each scale level that can be well approximated by white noise in the synthesis process.

Our computational scheme is based on an orthogonal P-band filter bank and a dyadic wavelet transform per channel. The P channels are tuned to the left and right sidebands of the harmonics so that sidebands are mutually independent. The structure computes the expansion coefficients of a new orthogonal and complete set of harmonic-band wavelets. The main point of our scheme is that we need only two parameters per harmonic in order to model the stochastic fluctuations of sounds from a pure periodic behavior.

Keywords and phrases: wavelets, $1/f$-noise, spectral modeling.

1. INTRODUCTION

The purpose of this work is to introduce a technique for the analysis and synthesis of pseudo-periodic signals based on a special kind of multiwavelet transform: the harmonic-band wavelet transform.

Long term correlation is detectable in a large class of pseudo-periodic signals such as voiced sounds in speech and music. These signals exhibit an approximate $1/f$ behavior in the neighborhood of each harmonic partial $f_n = nf_0$ (n integer), that is, a $1/|f - f_n|$ behavior. The power spectrum contains peaks, centered on the harmonics, whose shape is influenced by the long-term correlation of the stochastic fluctuations from the periodic behavior of the signal itself. From a perceptual point of view, these chaotic but correlated microfluctuations are relevant if one needs to emulate naturalness and dynamics of sounds with a detectable pitch.

Our idea is strongly inspired by the fact that $1/f$ processes arise not only in musical signals but also in many physical and biological systems as well as in man-made phenomena such as variations in traffic flow, economic data and fluctuation of pitch in music [1, 2]. These processes are significantly correlated at large time lags. Fractal models, such as fractional Brownian motion (fBm) [3], discrete fractional Gaussian noise (dfGn) or fractionally differenced Gaussian noise (fdGn) [4], are useful for representing systems or describing phenomena that are chaotic but strongly influenced by the past.

In a recent paper [5] Wornell introduced a new powerful method for the synthesis of $1/f$ stochastic processes by means of orthonormal wavelet bases. The main point is that, in order to obtain a good approximation of a given $1/f$ stochastic process, it is possible to adopt collections of mutually uncorrelated zero-mean processes with proper scale-dependent energy as wavelet synthesis coefficients. A single parameter is sufficient to control the slope of the $1/f$-shaped power spectrum. This parameter determines all the variances, that is, the energies of the synthesis coefficients for each different wavelet subband. Any random number generator can provide white noise coefficients.

Following Wornell's result we introduce a scheme for the analysis and synthesis of pseudo-periodic signals. In order to do this we need

(a) to define in a formal way a pseudo-periodic signal model, that is, the pseudo-periodic $1/f$-like noise,

(b) to define an appropriate mathematical tool for the analysis and the synthesis of this type of signals.

The theoretical effort of Section 3 is aimed at solving both problems by introducing a general cosine modulation and demodulation scheme. Thanks to this scheme we are able to provide a rigorous definition of the pseudo-periodic $1/f$-like noise, as well as to define the multichannel filter bank basis functions. The latter allow us to extend the class of multiplexed wavelet transforms [6, 7] by introducing the Harmonic-Band Wavelet Transforms (HBWT). We obtain a new form of wavelet transform that provides a well-suited tool for separating and analyzing the harmonics of sounds with a detectable pitch. Harmonic separation is performed by means of the cosine modulate multichannel filter banks. Each harmonic is then analyzed by means of a wavelet filter bank, according to Wornell's technique. Compared to the multiplexed wavelet transforms, the harmonic-band wavelets allow us to process each semiband of each partial independently.

As in Wornell's model, we show that it is possible to model the HBWT expansion coefficients of pseudo-periodic signals by means of white noise with suitable scale-dependent variances. These variances are the parameters controlling the shape of the spectrum, that is, the $1/f$-like behavior in the neighborhood of each harmonic partial.

The claim of our synthesis technique is that it allows one to control a highly complex stochastic process by means of relatively few parameters. Given a sound signal with a detectable pitch, we are able to grasp the essence of its evolution by means of perceptually relevant quantities. Roughly speaking, our scheme is a sort of additive synthesis in which instead of summing pure sinusoidal functions we add modulated fractal signals together.

For an overview on wavelet transforms and cosine modulated filter banks the reader is referred to the existing literature (see [8, 9, 10, 11, 12]).

The paper is organized as follows. In Section 2, we briefly review Wornell's result on the synthesis of $1/f$ processes by means of wavelet transforms. In Section 3, we define the pseudo-periodic $1/f$ noise process by means of a harmonic-band modulation and demodulation scheme. In Section 4, we illustrate the theoretical result on which our new method of synthesis is based. The proof of the main theorem is reported in Appendix A. In Section 5, we briefly review discrete-time harmonic-band wavelets and their properties. We also describe an operational scheme for the analysis and synthesis of pseudo-periodic $1/f$ noise. Section 6 illustrates applications to music synthesis. We provide results on harmonic-band wavelet analysis of real-life sounds and examples of the new method of synthesis. Finally, in Section 7 we draw our conclusions.

2. SYNTHESIS OF 1/f-NOISE BY MEANS OF DWT

In [5, Theorem 3] Wornell shows that, given an orthonormal wavelet basis $\psi_{n,m}(t)$ and a collection of mutually uncorrelated zero-mean synthesis coefficients $x_n(m)$ we obtain a process

$$x(t) = \sum_{n=-\infty}^{\infty} \sum_{m=-\infty}^{\infty} x_n(m)\psi_{n,m}(t) \qquad (1)$$

which is nearly $1/f$, that is, its time-averaged power spectrum

$$\bar{S}_x(\omega) = \sigma^2 \sum_{n=-\infty}^{\infty} 2^{\gamma n} \left| \Psi(2^n \omega) \right|^2 \qquad (2)$$

satisfies the relations

$$\frac{\sigma_{L,q}^2}{|\omega|^\gamma} \le \bar{S}_x \omega \le \frac{\sigma_{U,q}^2}{|\omega|^\gamma} \qquad (3)$$

for some $0 < \sigma_L^2 \le \sigma_U^2 < \infty$. The following autosimilarity relationship holds for any integer k:

$$|\omega|^\gamma S_x(\omega) = \left| 2^k \omega \right|^\gamma S_x(2^k \omega). \qquad (4)$$

In order to extend this result to pseudo-periodic signals, we will introduce a new set of multiwavelets. These multiwavelets are associated to a continuous-time filter bank with an infinite number of channels, whose outputs are sampled and analyzed by means of the Discrete-Time Wavelet Transform (DTWT).

For our developments we need a discrete-time counterpart of Wornell's results. It is easy to show that the discrete-time synthesis process

$$x(l) = \sum_{n=1}^{N} \sum_{m=-\infty}^{\infty} b_n(m)\psi_{n,m}(l) + \sum_{m=-\infty}^{\infty} a_N(m)\phi_{N,m}(l),$$
$$(5)$$

where $\phi_{N,0}(l)$ is the scaling sequence relative to the DTWT $\psi_{n,0}(l)$, is wide-sense cyclostationary (WSCS) of period 2^N with average power spectrum

$$\bar{S}_N(\omega) = \sum_{n=1}^{N} 2^{n\gamma} \frac{|\Psi_{n,0}(\omega)|^2}{2^n} + 2^{N\gamma} \frac{|\Phi_{N,0}(\omega)|^2}{2^N}. \qquad (6)$$

Here $\Psi_{n,0}(\omega)$ represents the DTFT of the wavelet sequence $\psi_{n,0}(l)$ and $\Phi_{n,0}(\omega)$ represents the DTFT of the corresponding scaling sequence $\phi_{n,0}(l)$.

Let $G(\omega)$ and $H(\omega)$ be the frequency responses of the QMF filters used to generate the discrete-time dyadic wavelets $\psi_{n,0}(l)$ as in [11]. They satisfy the relationships:

$$|G(\omega)|^2 + |H(\omega)|^2 = 2,$$
$$(7)$$
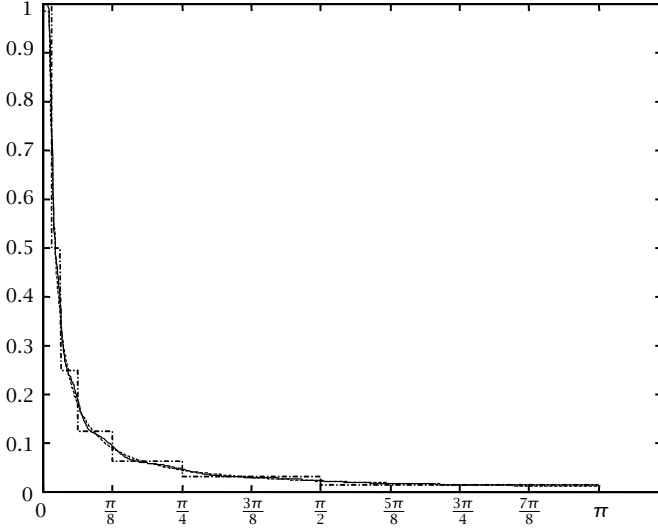$$H(\omega)G^*(\omega + \pi) + H^*(\omega + \pi)G(\omega) = 0.$$

FIGURE 1: $1/f$-like noise: synthesized by means of Daubechies wavelet (solid line), synthesized by ideals bandpass wavelets (dashed-dotted line) and ideal $1/f$ behaviour (dashed-line).

From this and the recursive definition of the DTWT, we have

$$\frac{\left|\Psi_{n,0}(\omega)\right|^2}{2^n} = \frac{\left|G(2^{n-1}\omega)\Phi_{n-1,0}(\omega)\right|^2}{2^n}$$
$$= \frac{\left|G(2^{n-1}\omega)\right|^2}{2}\prod_{r=0}^{n-2}\frac{\left|H(2^r\omega)\right|^2}{2}. \quad (8)$$

The spectrum in (6) is a multilevel approximation of a $1/f$ behavior as depicted in Figure 1. The accuracy of the approximation depends on the flatness and on the order of the filters. In the case where H and G are ideal filters, that is, for

$$H(\omega) = \begin{cases} \sqrt{2} & \text{if } -\dfrac{\pi}{2} < \omega < \dfrac{\pi}{2}, \\ 0 & \text{otherwise}, \end{cases} \quad (9)$$

and $G(\omega) = \sqrt{2} - H(\omega)$, we obtain from (8)

$$\frac{\left|\Psi_{n,0}(\omega)\right|^2}{2^n}$$
$$= \begin{cases} 1 & \text{for } \omega \in \left[\left(1-\dfrac{2^n-1}{2^n}\right)\pi, \left(1-\dfrac{2^{n-1}-1}{2^{n-1}}\right)\pi\right], \\ 0 & \text{otherwise}, \end{cases} \quad (10)$$

which yields a synthesized power spectrum

$$\bar{S}_N(\omega)$$
$$= 2^{N\gamma}\chi_{[0,(1-(2^N-1)/2^N)\pi]}(\omega)$$
$$+ \sum_{n=1}^{N} 2^{n\gamma}\chi_{[(1-(2^n-1)/2^n)\pi,(1-(2^{n-1}-1)/2^{n-1})\pi]}(\omega), \quad \omega > 0,$$
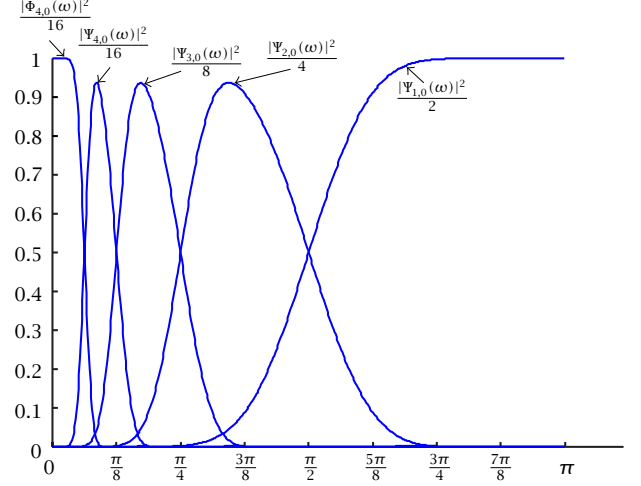$$(11)$$

FIGURE 2: Magnitude of the DTFT of the discrete-time scaled wavelets and order 4 scaling sequence based on Daubechies filters of order 11.

where

$$\chi_{[0,1]}(\omega) = \begin{cases} 1 & \text{for } 0 \le \omega \le 1 \\ 0 & \text{otherwise}. \end{cases} \quad (12)$$

This corresponds to the staircase function shown in Figure 1.

While staircase approximation adopting octave bands ideal filters has a pure demonstrative value, the approximation obtained by means of easily implementable Daubechies' filters provides a very accurate approximation of the spectrum as shown in Figure 1. This result can be appreciated from Figure 2, where we plot the magnitude DTFT of scaled Daubechies' wavelets of order 11.

The autosimilarity relation (4) does not carry over to discrete-time since the invariance for scale is only approximately true in that case.

3.   MODULATED $1/f$-NOISE

In this section we consider a general modulation and demodulation scheme that leads to a useful representation of pseudo-periodic processes. Based on this scheme we provide a definition of pseudo-periodic $1/f$-like noise suitable for the synthesis and the analysis of sounds.

3.1.   Harmonic-band modulation and demodulation

The frequency spectra of pseudo-periodic signals are characterized by harmonically spaced peaks at frequencies $\bar{\omega}k = 2\pi k/T_P$, where T_P is the average period of the signal. In order to separate the contribution of each of the harmonic bands, one can devise a set of ideal narrow-band filters of bandwidth $\Delta\omega = \pi/T_P$ each fitting a single sideband of the harmonics (see Figure 3). The magnitude of the Fourier transform of
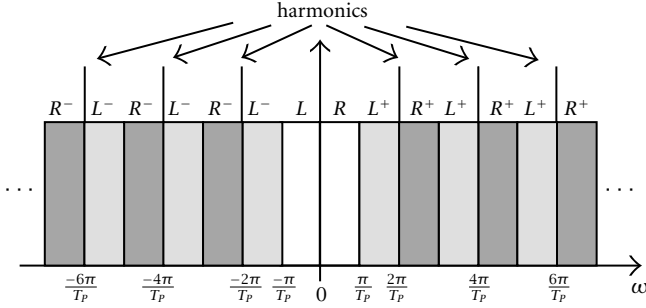
FIGURE 3: Harmonic subband allocation.

these filters is given by

$$H_q(\omega) = \begin{cases} \chi_{[q\pi/T_P,(q+1)\pi/T_P[}(\omega), & q \geq 0, \\ \chi_{]q\pi/T_P,(q+1)\pi/T_P]}(\omega), & q < 0, \end{cases} \quad (13)$$

where $q = 0, \pm 1, \pm 2, \ldots$, and

$$\chi_{[A,B[}(\omega) = \begin{cases} 1 & \text{if } A \leq \omega < B, \\ 0 & \text{otherwise} \end{cases} \quad (14)$$

is the characteristic function of the interval $[A, B[$. In our notation, the positive frequency right sideband R^+ of the kth harmonics corresponds to the band indexed by $q = 2|k|$. Its negative frequency companion, which we still denote as the right sideband R^-, is the band indexed by $q = -2|k| - 1$.

Similarly, positive and negative left sidebands, L^+ and L^-, are indexed, respectively, by $q = 2|k| - 1$ and $q = -2|k|$. Notice that for the d.c. component ($k = 0$) the bands R^- and L^-, respectively, coincide with the bands L^+ and R^+. The outputs of these filters may be baseband shifted, according to a suitable demodulation scheme. In dealing with real signals, it is convenient to combine positive and negative frequencies in such a way that the resulting component signal is still real. This is achieved by demodulating the output of each filter by the frequency of the corresponding harmonics, that is, by multiplying the band q signal by

$$\frac{1}{2} e^{-j(\lceil q/2 \rceil (2\pi/T_P)t + \beta_q)}, \quad (15)$$

where $\beta_q = \beta_{-q-1}$ are otherwise arbitrary phase factors. We then add together the outputs of the demodulated R^+ and R^-, and those of the demodulated L^+ and L^-. This results in the demodulation scheme reported in Figure 4. Considering couples of positive and symmetric negative bands, demodulation may be described as the projection $\langle K_q(t, \bullet), x(\bullet) \rangle$, $q = 0, 1, \ldots$, of a signal $x(t)$, where $\mathbf{K}_q$ is a set of real linear operators with kernels

$$K_q(t, \tau) = \frac{1}{T_P} \cos\left(\frac{t - (-1)^q (2q + 1)\tau}{2T_P} \pi + \beta_q\right) \\ \times \operatorname{sinc}\left(\frac{t - \tau}{2T_P}\right), \quad q = 0, 1, \ldots, \quad (16)$$

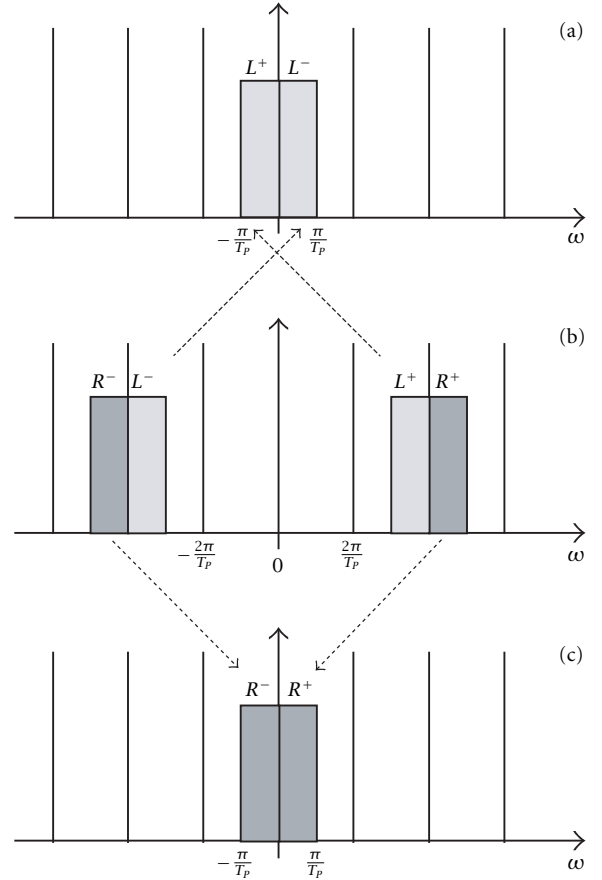where the sinc function represents ideal lowpass filtering,

FIGURE 4: Baseband shift of harmonic sidebands: (b) sidebands of the 2nd harmonics; (a) demodulation of the left sidebands; (c) demodulation of the right sidebands.

properly baseband demodulated by the cosine term. The operators described by the kernels (16) perform a harmonic cosine demodulation to baseband of the signal subband with frequency support in

$$W_q \equiv \left] \frac{-(q + 1)\pi}{T_P}, \frac{-q\pi}{T_P} \right] \cup \left[\frac{q\pi}{T_P}, \frac{(q + 1)\pi}{T_P} \right[. \quad (17)$$

The presence of the constant phase factors β_q allows us to generalize the cosine demodulation scheme to other schemes, such as sine demodulation. We denote by $\mathbf{V}_q$ the L^2 subspace of signals bandlimited to W_q. The operator $\mathbf{K}_q$ defines an isomorphism $\mathbf{V}_q \leftrightarrow \mathbf{V}_0$, where $\mathbf{V}_0$ is the space of bandlimited baseband signals, with frequency support in $] - \pi/T_P, \pi/T_P[$. In fact, one can verify that $\mathbf{K}_q$ is invertible, with inverse kernel $K_q^{-1}(t, \tau) = K_q(\tau, t) = K_q^\dagger(t, \tau)$, where the symbol $\dagger$ denotes the adjoint. Hence $\mathbf{K}_q$ is unitary. Conversely, the operators $\mathbf{K}_q^{-1}$ perform a harmonic cosine modulation, repositioning the demodulated subband to the domain (17). It should be noted that, unless $q = 0$, domain and range space of the operator are different. Thus, $\mathbf{K}_q$ and $\mathbf{K}_q^{-1}$ do not commute, rather the domain and range space
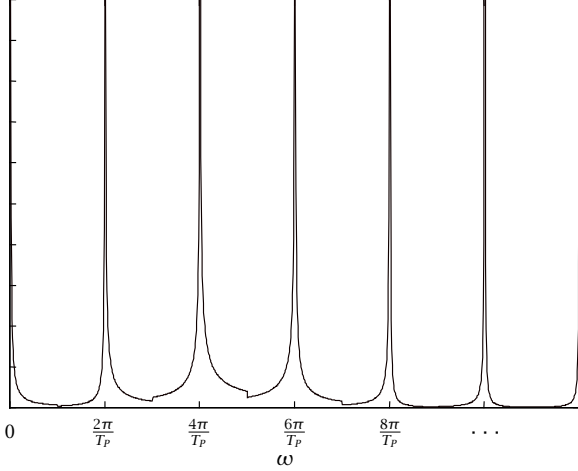
FIGURE 5: Model pseudo-periodic power spectrum.

of $\mathbf{K}_q^{-1}\mathbf{K}_q$ is $\mathbf{V}_q$, while the domain and range space of $\mathbf{K}_q\mathbf{K}_q^{-1}$ is $\mathbf{V}_0$. Also, the identity operator in $\mathbf{V}_q$ has kernel $I_q(t,\tau) = (1/T_P)\cos((2q+1)\pi(t-\tau)/2T_P)\operatorname{sinc}((t-\tau)/2T_P)$, which, for $q = 0$, corresponds to $I_0(t,\tau) = (1/T_P)\operatorname{sinc}((t-\tau)/T_P)$.

Harmonic cosine modulation and demodulation is the main ingredient of our representation and formal definition of pseudo-periodic signals.

3.2. Pseudo-periodic $1/f$-like noise

We model acoustic pseudo-periodic signals with fundamental frequency $f_0 = \omega_0/2\pi$ by means of a superposition of cosine modulated bandlimited $1/f$ processes. Each process contributes to a single side band of one of the harmonics of a pseudo-periodic signal. Each one of these $1/f$ processes is characterized by two parameters σ and γ (see equation (2)). The parameter σ controls the global energy of the process, while the parameter γ controls the slope of the spectral curve. In the pseudo-periodic case we denote each harmonic partial by means of the index k and we distinguish between the left and right sideband by means of the indexes L and R, respectively. We obtain a set of parameters $\sigma_{k,R}^2$ and $\sigma_{k,L}^2$, corresponding to the amplitudes of the side bands of the harmonics k and a set of parameters $\gamma_{k,R}$ and $\gamma_{k,L}$ controlling the slope of their $1/f$-like spectra.

An example of pseudo-periodic spectrum is shown in Figure 5. The modulating frequencies are chosen to be harmonically related. The bandwidth B of each process equals half the harmonic spacing, that is, $B = \omega_0/2$.

In other words, the average spectrum of the model process has the following form:

$$S(\omega) = \sum_{q=0}^{\infty} \frac{\sigma_{q,R}^2}{|\omega - q\omega_0|^{\gamma_{q,R}}} \chi_{[q\omega_0,(q+1/2)\omega_0[}(\omega)$$
$$+ \frac{\sigma_{q,L}^2}{|\omega - q\omega_0|^{\gamma_{q,L}}} \chi_{[(q-1/2)\omega_0,q\omega_0[}(\omega), \quad \omega \geq 0. \tag{18}$$

We can provide a formal definition of pseudo-periodic $1/f$-like noise that extends that of the $1/f$ noise given in [5]. In fact, if each sideband of the harmonics is baseband shifted by means of cosine demodulation, as described in the previous section, the resulting process is $1/f$, bandlimited to $[-\omega_0/2, \omega_0/2]$. This is equivalent to say that, by passing the demodulated component processes through an ideal band-pass filter

$$H^{(\varepsilon)}(\omega) = \chi_{[-\omega_0/2,-\varepsilon]}(\omega) + \chi_{[\varepsilon,\omega_0/2]}(\omega), \tag{19}$$

where ε is arbitrarily small, one obtains a finite-variance wide-sense stationary process. This is actually the main idea of the definition of $1/f$ in [5]. Therefore, we can provide the following definition.

Definition 1. A stochastic process $x(t)$ is said to be a $1/f$-like pseudo-periodic noise if there exists a $T_P > 0$ such that when $x(t)$ is operated by $\mathbf{K}_q$ in (13) it yields a collection of processes

$$w_q(t) = \int_{-\infty}^{\infty} K_q(t,\tau)x(\tau)\,d\tau, \quad q = 0,1,\dots \tag{20}$$

which, when filtered through $H^{(\varepsilon)}(\omega)$, with $\omega_0 = 2\pi/T_P$, become wide-sense stationary and bandlimited processes with power spectrum

$$S_{w_q}(\omega) = \begin{cases} \dfrac{\sigma_q^2}{|\omega|^{\gamma_q}} & \text{if } \varepsilon < |\omega| < \dfrac{\omega_0}{2}, \\ 0 & \text{otherwise}, \end{cases} \tag{21}$$

for some γ_q and σ_q.

The operations involved in (20) are equivalent to filtering the single sidebands of each of the harmonics, separately for the positive and negative frequencies, and properly baseband shifting the result. The phase factors β_q in (16) are arbitrary. It can be shown that the power spectrum $S_{w_q}(\omega)$ does not depend on the choice of β_q. Similarly, any signal generated by harmonic modulation of a $1/f$ baseband process with arbitrary phase yields a $1/f$ process when demodulated by means of (20).

This is true even if the phase factors do not coincide. Therefore, our definition is consistent.

Comparing (21) with the model spectrum in (18), we can make the following associations:

$$\begin{aligned} \gamma_{2q-1} &= \gamma_{q,L}, & \gamma_{2q} &= \gamma_{q,R}, \\ \sigma_{2q-1} &= \sigma_{q,L}, & \sigma_{2q} &= \sigma_{q,R}. \end{aligned} \tag{22}$$

Since the resulting processes $w_q(t)$ in Definition 1 are bandlimited to $[-\omega_0/2, \omega_0/2]$, they can be sampled with sampling rate $\omega_0/2\pi = 1/T_P$. It can be shown that the operations in (20) followed by sampling at a rate $1/T_P$ are equivalent to the projection of $x(t)$ on the set of functions $\{g_{q,k}(t)\}_{q=0,1,\dots;k\in\mathbb{Z}}$, defined as follows:

$$g_{q,k}(t) = g_{q,0}(t - kT_P) \tag{23}$$

with

$$g_{q,0}(t) = \frac{1}{\sqrt{T_P}} \cos\left(\frac{2q+1}{2T_P}\pi t\right) \operatorname{sinc}\left(\frac{t}{2T_P}\right). \qquad (24)$$

The set in (23) is easily shown to form an orthonormal basis. The functions $g_{q,0}(t)$ are the impulse responses of ideal bandpass filters, with passband (17), that is, the $\operatorname{sinc}(t/2T_P)$ ideal lowpass filter with passband $]-\pi/T_P, \pi/T_P[$, modulated to the band (17) by the cosine function. It is clear that the coefficient obtained by projecting a signal $x(t)$ on a basis element $g_{q,k}(t)$, where k corresponds to the time kT_P and q corresponds to the band (17), is just the sample at time kT_P of the component of $x(t)$ bandlimited to (17), that is, $\langle x, g_{q,k} \rangle = \sqrt{T_P} w_q(kT_P)$.

4. SYNTHESIS OF PSEUDO-PERIODIC 1/f-LIKE NOISE BY MEANS OF HARMONIC-BAND WAVELET TRANSFORM

In order to extend Wornell's results to the synthesis of $1/f$ pseudo-periodic processes by means of wavelet bases, and to introduce their discrete-time counterpart we need the following lemma.

Lemma 1. *A stochastic process $x(t)$ defined as follows:*

$$x(t) = \sum_{q=0}^{\infty} \sum_{k=-\infty}^{\infty} v_q(k) g_{q,k}(t), \qquad (25)$$

where the $g_{q,k}(t)$ are given in (23) and $\{v_q(k)\}$ are jointly stationary discrete-time stochastic processes, that is, $R_{v_q,v_{q'}}(k,k') = R_{v_q,v_{q'}}(k-k')$, is wide sense cyclostationary (WSCS) with period T_P.

Proof. We have

$$R_x(t + rT_P, t' + rT_P)$$
$$= E\left\{\left(\sum_{q=0}^{\infty} \sum_{k=-\infty}^{\infty} v_q(k) g_{q,k}(t + rT_P)\right)\right.$$
$$\left.\times \left(\sum_{q'=0}^{\infty} \sum_{k'=-\infty}^{\infty} v_{q'}(k') g_{q',k'}(t' , rT_P)\right)\right\} \qquad (26)$$

which, by making the substitutions $k' - k = l$ and $r - k = k''$ and using (23) becomes

$$R_x(t + rT_P, t' + rT_P)$$
$$= \sum_{q,q'=0}^{\infty} \sum_{l,k''=-\infty}^{\infty} g_{q,0}(t - k''T_P)$$
$$\times g_{q',0}(t' - (l + k'')T_P) R_{v_q,v_{q'}}(l) \qquad (27)$$
$$= R_x(t,t'),$$

which does not depend on r. $\qquad \square$

We now introduce a continuous time multiwavelet basis forming the harmonic-band wavelet set:

$$\xi_{n,m,q}(t) = \sum_r \psi_{n,m}(r) g_{q,r}(t), \qquad (28)$$

where $n \in N$, $m \in Z$, $q = 0, 1, \ldots, P$, $P \in N$ and $\{\psi_{n,m}(r)\}_{n \in N, m \in Z}$ is an ordinary discrete-time wavelet basis while $g_{q,r}(t)$ are defined in (19).

The Fourier transforms of the harmonic-band wavelets correspond to comb versions of ordinary wavelets, filtered by the filterbank with frequency responses $G_{q,0}(\omega)$:

$$\Xi_{n,m,q}(\omega) = \Psi_{n,m}(T_P \omega) G_{q,0}(\omega). \qquad (29)$$

In (29) $G_{q,0}(\omega)$ is the Fourier transform of $g_{q,0}(t)$ and $\Psi_{n,m}(T_P \omega)$ is the Fourier transform of a Comb wavelet [6]. This means that we have infinite comb wavelets, one for each q, and that the action of filtering is essentially equivalent to selecting a single sideband of the harmonics. What we have obtained is to wavelet transform each single sideband independently. Furthermore, the harmonic-band wavelets (28) satisfy the following shift covariance property:

$$\xi_{n,m,q}(t + 2^N rT_P) = \xi_{n,m-2^{N-n}r,q}(t). \qquad (30)$$

Consider the case where the $\{v_q(k)\}$ in (25) are WSCS processes with period $2^N P$ (see also (5)) defined as follows:

$$v_q(r) = \sum_{n=1}^{N} \sum_{m=-\infty}^{\infty} \beta_q^{n/2} v_q^n(m) \psi_{n,m}(r), \qquad (31)$$

where the $v_q^n(m)$ are unit variance mutually uncorrelated coefficients, while $\beta_q = \sigma_q^2 2^{\gamma_q}$ are scale dependent energy factors. We can prove the following lemma.

Lemma 2. *A stochastic process $x(t)$ such that*

$$x(t) = \sum_{q=0}^{\infty} \sum_{k=-\infty}^{\infty} v_q(k) g_{q,k}(t)$$
$$= \sum_{q=0}^{\infty} \sum_{n=1}^{N} \sum_{m=-\infty}^{\infty} \beta_q^{n/2} v_q^n(m) \xi_{n,m,q}(t), \qquad (32)$$

where the $\xi_{n,m,q}(t)$ are defined in (28), is cyclostationary with period $2^N T_P$.

Proof. We have

$$R_x(t + 2^N rT_P, t' + 2^N rT_P)$$
$$= E\left\{\left(\sum_{q=0}^{\infty} \sum_{n=1}^{N} \sum_{m=-\infty}^{\infty} \beta_q^{n/2} v_q^n(m) \xi_{n,m,q}(t + 2^N rT_P)\right)\right.$$
$$\left.\times \left(\sum_{q'=0}^{\infty} \sum_{n'=1}^{N} \sum_{m'=-\infty}^{\infty} \beta_q^{n'/2} v_{q'}^{n'}(m') \xi_{n',m',q'}(t' + 2^N rT_P)\right)\right\}. \qquad (33)$$

By using (23), the shift property (30) and the fact that

$R_{v_{n,q}, v_{n',q'}}(m, m') = \beta_q^n \delta_{n,n';q,q';m,m'}$, equation (33) becomes

$$R_x(t + 2^N r T_P, t' + 2^N r T_P)$$
$$= \sum_{q=0}^{\infty} \sum_{n=1}^{N} \sum_{m=-\infty}^{\infty} \beta_q^n \xi_{n, m-2^{N-n}r, q}(t) \xi_{n, m-2^{N-n}r, q}(t'). \tag{34}$$

Finally, by the substitution $m' = m - 2^{N-n}r$ we obtain

$$R_x(t + 2^N r T_P, t' + 2^N r T_P)$$
$$= \sum_{q=0}^{\infty} \sum_{n=1}^{N} \sum_{m'=-\infty}^{\infty} \beta_q^n \xi_{n,m,q}(t) \xi_{n,m,q}(t') = R_x(t,t') \tag{35}$$

which is independent of r.

The same result holds for the scale residue in (5). □

We are then able to derive the following result for the synthesis.

Proposition 1. *Consider an orthonormal set of functions $\{g_{q,k}(t)\}_{q=0,1,\dots;k\in\mathbb{Z}}$, as defined in (23) and a collection of jointly uncorrelated sets of coefficients $\{v_q(k)\}_{q=0,1,\dots}$, related to (5) by the following relation:*

$$v_q(k) = \frac{1}{\sqrt{T_P}} x(k)$$
$$= \frac{1}{\sqrt{T_P}} \left(\sum_{n=1}^{N} \sum_{m=-\infty}^{\infty} b_{n,q}(m) \psi_{n,m}(k) \right. \tag{36}$$
$$\left. + \sum_{m=-\infty}^{\infty} a_{N,q}(m) \phi_{N,m}(k) \right),$$

where $\{b_{n,q}(m)\}$ and $\{a_{N,q}(m)\}$ are jointly uncorrelated WSS white noise processes with variances $\mathrm{Var}\{b_{n,q}(m)\} = \sigma_q^2 2^{n\gamma_q}$ and $\mathrm{Var}\{a_{n,q}(m)\} = \sigma_q^2 2^{N\gamma_q}$. Then the random process

$$s(t) = \sum_{q=0}^{\infty} \sum_{m=-\infty}^{\infty} v_q(m) g_{q,m}(t), \tag{37}$$

has an average power spectrum of the form

$$\bar{S}(\omega) = \frac{1}{T_P} \sum_{q=0}^{\infty} \sigma_q^2 |G_{q,0}(\omega)|^2$$
$$\times \left(\sum_{n=1}^{N} 2^{n\gamma_q} |\Psi_{n,0}(\omega T_P)|^2 + 2^{N\gamma_q} |\Phi_{n,0}(\omega T_P)|^2 \right). \tag{38}$$

For the proof see Appendix A.
In the ideal case

$$|G_{q,0}(\omega)|^2$$
$$= (\chi_{]-(q+1)\pi/T_P, -q\pi/T_P]}(\omega) + \chi_{[q\pi/T_P, (q+1)\pi/T_P[}(\omega)) \tag{39}$$
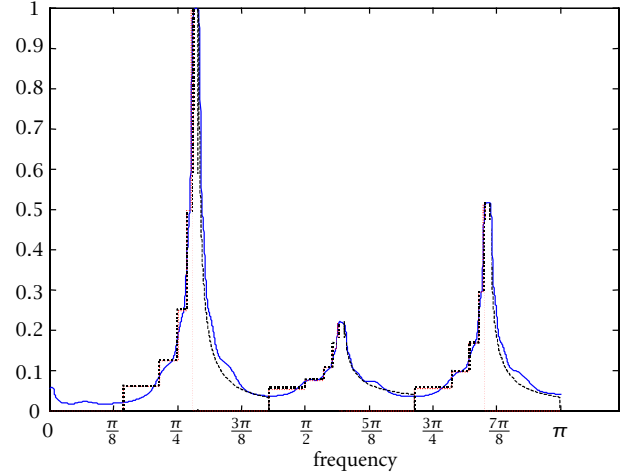

FIGURE 6: Synthesized pseudo-periodic $1/f$-like noise: three harmonics with different σ_q and γ_q. (a) solid line: synthesized by DCT and Daubechies wavelet (b) dotted line: synthesized by ideal filter banks (c) dashed line: ideal spectrum behaviour.

and (38) is approximately $1/f$ near each harmonic $2l(\pi/T_P)$ with $k = \lfloor (q+1)/2 \rfloor$, $q = 0, 1, \dots$.

That is, for

$$(2l - 1) \frac{\pi}{T_P} \le \omega \le 2l \frac{\pi}{T_P} \quad \text{if } q \text{ is odd (right semiband)}, \tag{40}$$

or

$$2l \frac{\pi}{T_P} \le \omega \le (2l+1) \frac{\pi}{T_P} \quad \text{if } q \text{ is even (left semiband)}, \tag{41}$$

we have

$$\frac{\sigma_{L,q}^2}{|\omega - 2l(\pi/T_P)|^{\gamma_q}} \le \bar{S}_N(\omega) \le \frac{\sigma_{U,q}^2}{|\omega - 2l(\pi/T_P)|^{\gamma_q}} \tag{42}$$

for some $0 < \sigma_{L,q}^2 \le \sigma_{U,q}^2 < \infty$.

It follows from Proposition 1 that one can synthesize a signal with an approximately pseudo-periodic $1/f$-like behavior, as shown in Figure 6.

This is the main result of our scheme. The inverse harmonic-band wavelet transform with random coefficients is used as a synthesis scheme for pseudo-periodic $1/f$-like noise. We are able to simulate a real-life pseudo-periodic signal with arbitrary pitch P. The parameters necessary to define the behavior of each sideband are only two: σ_q and γ_q. They control, respectively, the amplitude and the slope of the sideband spectrum.

5. DISCRETE-TIME HARMONIC-BAND WAVELETS

The discrete-time counterpart of (23) is the basis associated with an ideal P band filterbank, where P is the length in samples of the period of the pseudo-periodic signal. In order to obtain an efficient scheme for the analysis and synthesis of pseudo-periodic $1/f$ noise we consider an approximation of the ideal filterbank by a perfect reconstruction structure [12].
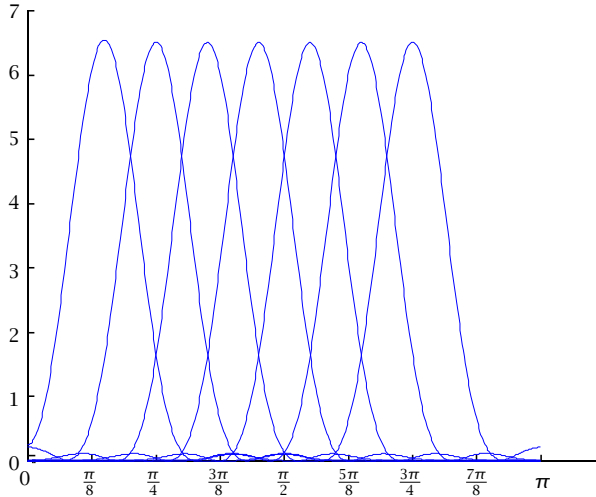
FIGURE 7: Magnitude of the DTFT of the cosine modulated filters (28).

FIGURE 8: Magnitude Fourier transform of harmonic-band wavelet.

In particular, we consider the class of type IV cosine modulated bases, whose Fourier transform magnitude is shown in Figure 7

$$h_{q,r}(l) = h_{q,0}(l - rP), \quad q = 0, \ldots, P - 1; \; r \in \mathbb{Z},$$

$$h_{q,0}(l) = W(l) \cos\left(\frac{2q+1}{2P}\left(l - \frac{M-1}{2}\right)\pi - (-1)^q \frac{\pi}{4}\right),$$
(43)

where the length M lowpass prototype impulse response $W(l)$ satisfies the symmetry conditions given in [13]. That is, for even P

$$W(l) = W(2P - l - 1) \quad \text{for } l = 0, \ldots, 2P - 1, \quad (44)$$

$$W^2(l) + W^2(P - l - 1) = 2 \quad \text{for } l = 0, \ldots, P - 1, \quad (45)$$

$$W(l) = 0 \quad \text{for } l < 0, \; l > 2P - 1. \quad (46)$$

For odd P, (45) is replaced by

$$W^2(l) + W^2(P - l - 1) = 2 \quad \text{for } l = 0, \ldots, P - 1, \; l \neq \frac{P-1}{2},$$

$$W\left(\frac{P-1}{2}\right) = 1 \quad \text{for } l = \frac{P-1}{2}.$$
(47)

A straigthforward computation shows that the conditions of orthogonality and completeness of harmonic-band wavelets are satisfied. In other words,

$$\frac{1}{P} \sum_{l=-\infty}^{\infty} W(l - rP)W(l - r'P)$$

$$\times \cos\left(\frac{2q+1}{4P}(2(l - rP) - P + 1)\pi\right)$$

$$\times \cos\left(\frac{2q'+1}{4P}(2(l - r'P) - P + 1)\pi\right) = \delta_{k,k'}\delta_{r,r'}$$
(48)

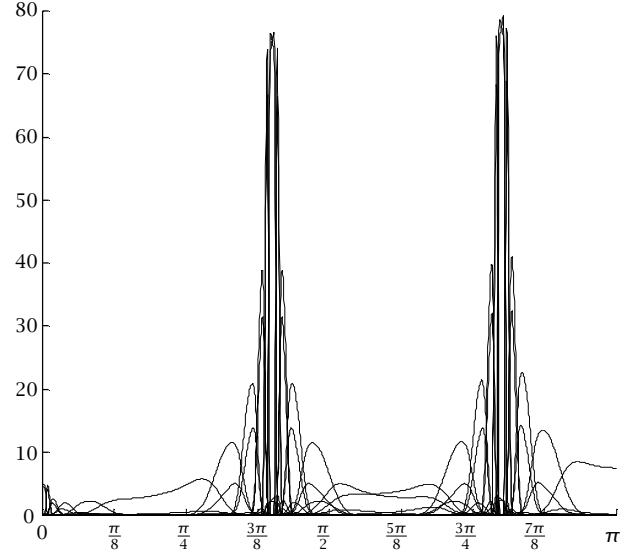for orthogonality, while for completeness we have

$$\frac{1}{P} \sum_{r=-\infty}^{\infty} \sum_{q=0}^{P-1} W(l - rP)W(l' - rP)$$

$$\times \cos\left(\frac{2q+1}{4P}(2(l - rP) - P + 1)\pi\right)$$

$$\times \cos\left(\frac{2q+1}{4P}(2(l' - rP) - P + 1)\pi\right) = \delta_{l,l'}.$$
(49)

In order to synthesize the samples of $1/f$-like processes $w_q(k)$, we adopt the discrete-time counterpart of the scheme illustrated in Section 2. The overall structure is realized by introducing the discrete-time harmonic-band wavelets and the synthesis is achieved by using white noise coefficients. The discrete-time harmonic-band wavelets are defined by

$$\xi_{n,m,q}(k) = \sum_r \psi_{n,m}(r)h_{q,r}(k),$$

$$n = 1, 2, \ldots, N; \; m \in \mathbb{Z}; \; q = 0, 1, \ldots, P - 1,$$
(50)

where $\psi_{n,m}(r)$ are discrete-time ordinary wavelets [8] and $h_{q,r}(k)$ are the cosine modulated functions (43). The DTFT of the basis elements (50) are shown in Figure 8.

A structure for computing the discrete-time harmonic-band wavelet transform and its inverse is shown in Figure 9, where the blocks WT denote wavelet transform and the blocks IWT denote its inverse.

In the analysis structure, the signal is sent to a P channel filterbank separating the semibands. In view of perfect reconstruction, the output can then be downsampled by P. Each P-downsampled signal is then wavelet transformed (WT block). Signal reconstruction is achieved by separately inverse wavelet transforming the harmonic-band wavelet coefficients and passing these sequences through the inverse P channel
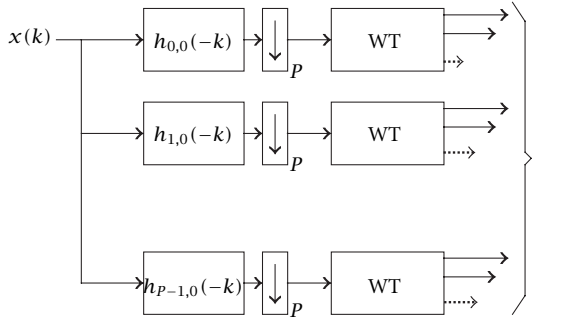
(a) Harmonic band wavelet coefficients.
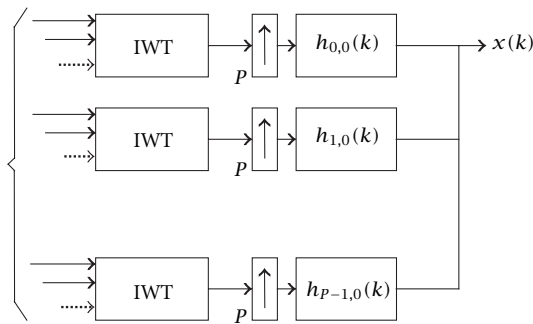
(b) Harmonic band wavelet coefficients.

FIGURE 9: Harmonic-band wavelet transform: (a) analysis and (b) synthesis structures.

FIGURE 10: Spectral subdivision, dotted: deterministic component, gray: pseudo-periodic $1/f$-like model, dark gray: shot noise model.

filterbank with upsampling factor P. Upsampling moves the spectrum of each subsignal back to its proper subband.

The harmonic-band wavelets generalize the Multiplexed Wavelets (MW), recently introduced in [6, 7], to which they revert when $h_{q,0}(k) = \delta(k)$, where $\delta(k)$ is the unit pulse sequence. Similarly to the MW, harmonic-band wavelets are useful for separating, for each harmonics, the sinusoidal behavior (scaling component) from transients and noise (wavelet components). The idea of our model is to employ the theoretical result of Proposition 1 in order to have an efficient scheme for synthetically reproducing the noisy sidebands of the spectrum of voiced sounds in music. Experimental results confirm the validity of the $1/f$ model for the sidebands in a wide class of musical pseudo-periodic signals. Thanks to the result of Proposition 1 we can easily reproduce the synthesis coefficients in our scheme by means of white noise or weakly correlated noise. The coefficient energy is controlled by few parameters (2 per each semiband) drawn from the analysis scheme of the signal.

6. APPLICATIONS TO MUSIC SYNTHESIS

The results of Section 3 are useful for the synthesis of the stochastic microfluctuations of the steady part of sounds.
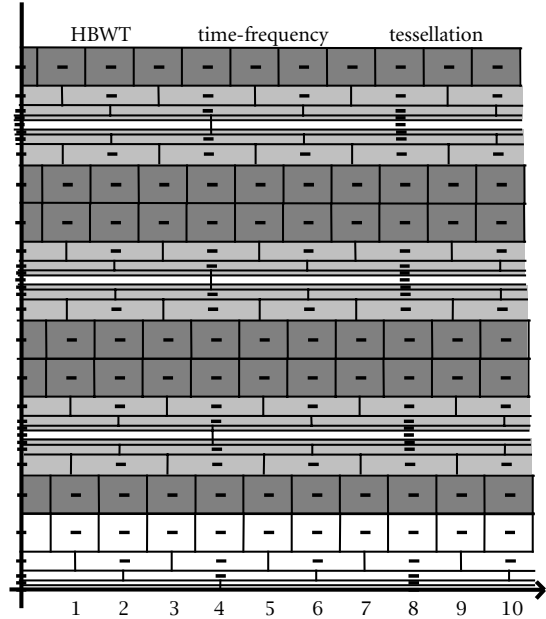
That is, we are able to synthesize the part of the power spectrum of a pseudo-periodic sound that is well represented by means of a pseudo-periodic $1/f$-like model. In other words, the harmonic-band wavelet subbands of each harmonic peak are well suited to represent the stochastic fluctuations with respect to the harmonic components. In Figure 10 this part of the spectrum is shadowed in gray and corresponds to the 2nd, 3rd, and 4th harmonic-band wavelet subbands. The deterministic component, corresponding to the dotted areas in Figure 10, is represented by the scaling component. We just resynthesize it from the set of analysis coefficients in order to maintain the time coherence of the harmonic part of the original sounds. In view of the downsampling factor 2^N this requires only few samples.

From an auditory point of view, the HBWT subbands contain all the information relative to the timbre dynamic, that is, the "life" of sound. By means of our technique a separation of the harmonic peaks and the stochastic components is straightforward. The perfectly reconstructed harmonic components sound clearly "poor" and unnatural to our ear. Thus the reproduction of the harshness of the stochastic components is essential to provide a sound with a convincing, natural "flavor."

In our experiments, we verified that not all the sidebands of the harmonics are representable by a $1/f$-like model. In particular all the first wavelet subbands do not fit the model (see Figure 10, dark gray areas). These are the bands containing the extra noise due to the physical device of production of sound, or, more precisely, the bands where this type of noise is not masked. This noise shows a long time correlation due to all the discontinuities present for example in breath noise or

bow noise in string instruments. Other techniques seem to be more suitable in order to deal with this time correlation due to all the discontinuities present for example in breath noise or bow noise in string instruments. Other techniques seem to be more suitable in order to deal with this time correlation, one of these being shot noise models.

The synthesis technique for the pseudo-periodic $1/f$-like model requires the estimation of three parameters per each harmonic partial $k : \sigma_k, \gamma_{k,R}, \gamma_{k,L}$. The meaning of these parameters is intuitively appealing. Figure 6 depicts three harmonics of pseudo-periodic signal. We use identical variances for the left and right semibands of each harmonics. The parameters σ_k control the amplitude of the kth harmonic, while the parameters $\gamma_{k,R}$ and $\gamma_{k,L}$ control the $1/f$-like slopes respectively of the right and left semiband of kth harmonic. The parameters σ_k may be estimated from the frequency spectrum by means of peak-picking algorithm. The estimation of the γ's is based on the results of the HBWT analysis. Each subband is a piecewise approximation of a $1/f$ spectral curve as shown in Figure 6. Considering the logarithm of the energies of each of the subbands of a single sideband, we find a linear relationship characterized by the parameter γ_k. More specifically, we can perform the following linear regression:

$$\log_2\left(\mathrm{Var}\left(x_{n,q}(m)\right)\right) = \gamma_q n + \mathrm{const}, \qquad (51)$$

where $k = \lfloor (q + 1)/2 \rfloor$ is the kth harmonic and $x_{n,q}(m) = \sum_k x(k)\xi_{n,m,q}(k)$ are the analysis sequences at the different subbands n. The lower the parameter γ the higher the energy and the presence of the stochastic components and vice versa.

The first experiment we performed was a test of the limitations of the pseudo-periodic $1/f$ model. We considered different wind instruments (clarinet, trumpet, oboe, bassoon) and bow instruments (cello and violin) and we applied (51). What comes out is that the first wavelet subband and the subbands of the resolution higher than the fifth are not fitting the $1/f$ model (see Figure 11 as an example in the case of a trumpet). We conclude that only four or three subbands, depending on the instrument, are well representable by means of the $1/f$ pseudo-periodic model. As already discussed, the first subbands mainly contain additional noise due to the physical excitation system and their energy is higher than that provided by the $1/f$ slope. This appear as a background noise, different from the stochastic fluctuations with respect to a periodic behavior. This noise is masked (but present) in the proximity of the harmonic peaks. On the contrary it stands out in the first HBWT spectral subbands, where it may overlap the pseudo-periodic $1/f$ spectral behavior. For this portion of the spectrum another model has to be devised. The noise contained in these bands can be modeled by means of LPC techniques.

The higher subbands (the fifth in Figure 11) contain the harmonic part and all the information concerning the time envelope. In order to preserve the time coherence in the harmonics we employ the full set of HBWT analysis coefficients, which are actually the $2^{-5} = 1/32$ part of the original sound samples.
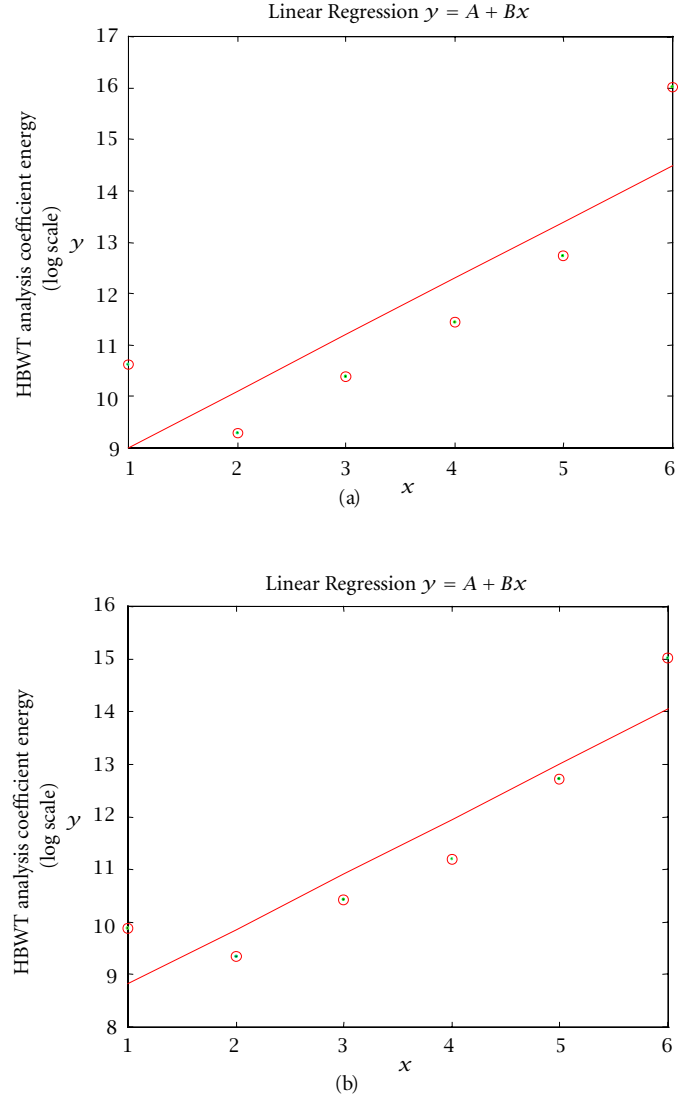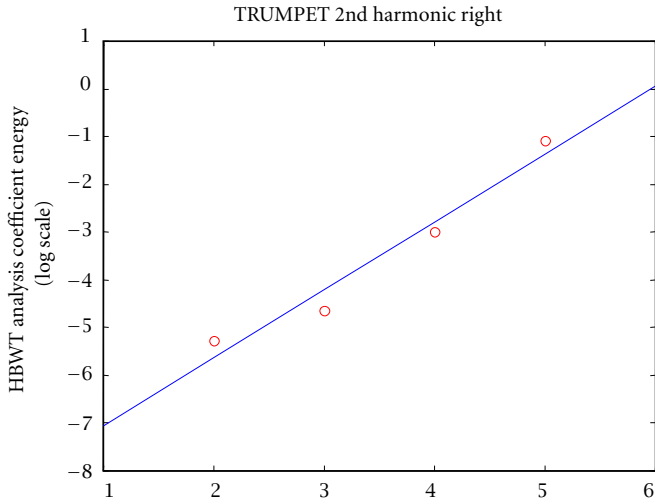

FIGURE 11: Trumpet: linear regression according to (33), (a) first harmonic left sideband, (b) right sideband.
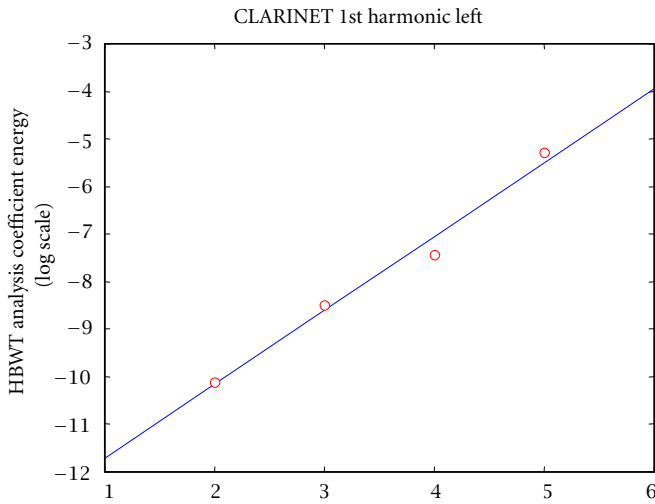
A further problem is the transient, that is, the sound attack, fundamental for the perception of timbre. Also in this case we retain the original analysis HBWT coefficients.

The whole method consists then in preserving some subsets of the HBWT analysis coefficients and in generating other subsets by employing a restricted set of parameters (see Figure 10).
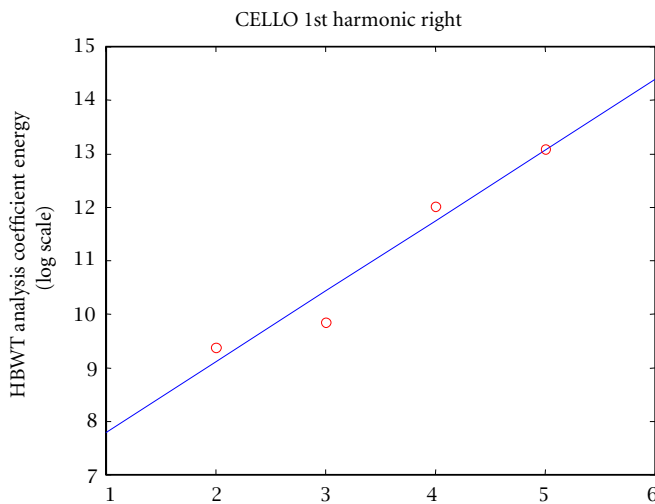
From the experimental results shown in Figure 12, it is possible to see how the pseudo-periodic $1/f$-like model is well suited for representing the inner subbands, that is, the 2nd, 3rd, 4th, and 5th subbands. These results show that we are able to synthesize sounds with the same power spectra as the original sounds. In Figures 14, 15, 16, 17, 18, and 19, we show the results of the resynthesis of an oboe, a trumpet and a flute. From an acoustical point of view (going beyond

TRUMPET 2nd harmonic right

(a) Wavelet scales.

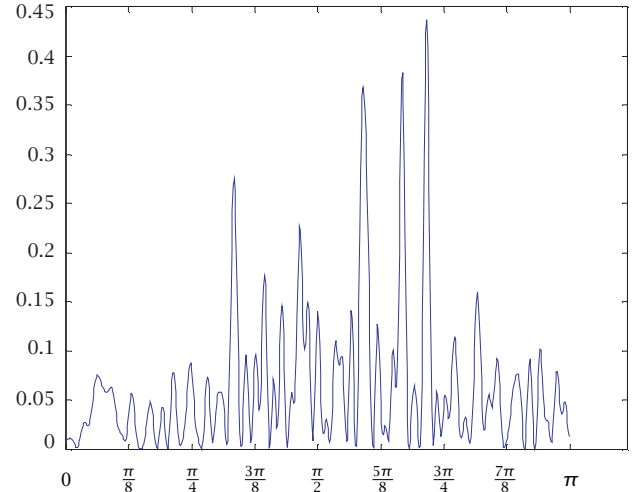CLARINET 1st harmonic left

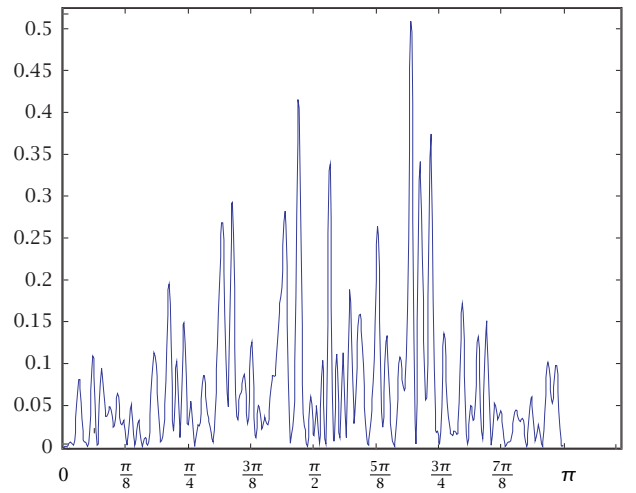(b) Wavelet scales.

CELLO 1st harmonic right

(c) Wavelet scales.

FIGURE 12: Results of the application of (33) to the HBWT analysis coefficients of three different instruments (2nd, 3rd, 4th, and 5th subbands). Correlation coefficients: (a) 0.9790 (b) 0.9911 (c) 0.9739.

(a) Magnitude Fourier transform of analysis coefficients of one subband of a trumpet.

(b) Magnitude Fourier transform of synthesis coefficients reproduced by means of AR techniques.

FIGURE 13

the mere spectral magnitude matching), some refinements are necessary. The white noise coefficient approximation provides a good equilibrium between the energy of the harmonic components and the stochastic ones. Nevertheless by means of white noise we obtain something that sounds as "properly energy-scaled white noise." Some kind of coefficient pre-filtering, that is, white noise coloring is thus necessary. The starting point is again Wornell results in [5]. He showed that the analytical wavelet coefficients of a 1/*f* process have a small but nonzero correlation. In order to simulate that correlation we apply LPC analysis to the HBWT coefficients. The resulting AR (autoregressive) filters are employed in the resynthesis, in order to color the rough white noise coefficients (see Figure 13). The different "order" of acoustical quality obtained by means of this technique is clearly audible. If we compare each perfectly reconstructed subband with
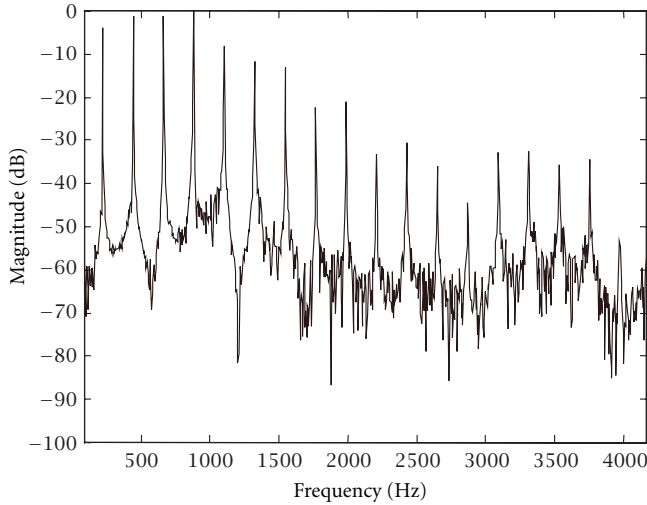
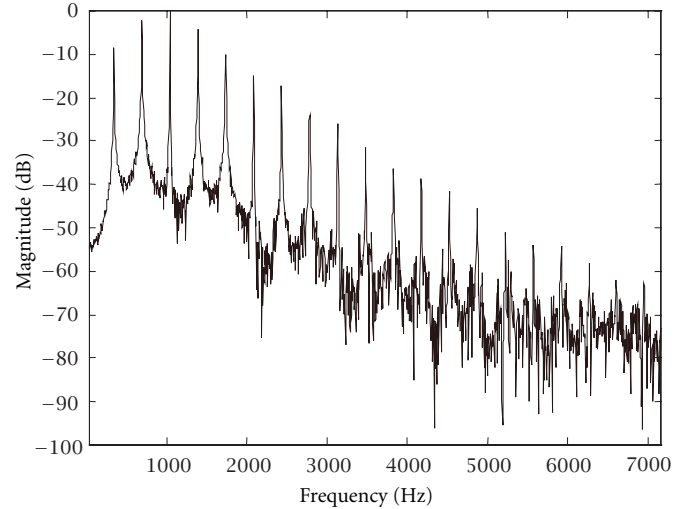FIGURE 14: Real-life oboe (287.5 Hz).
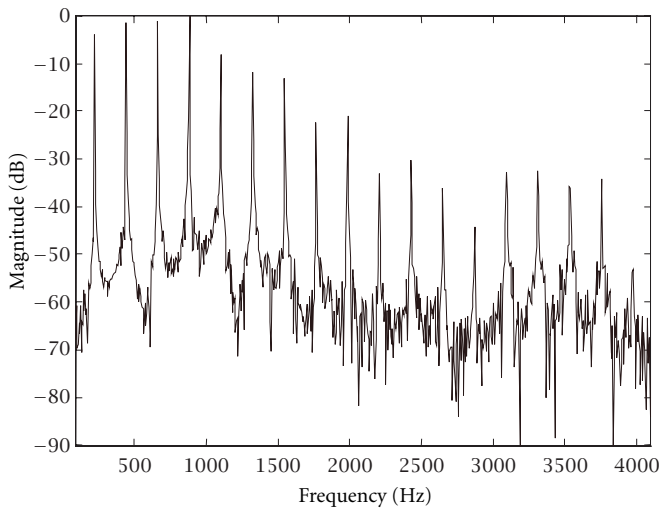

FIGURE 16: Real-life trumpet (347 Hz).

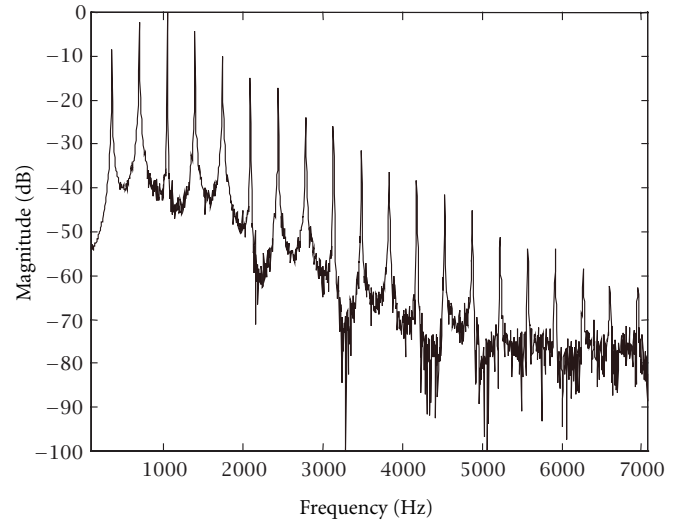

FIGURE 15: Synthesized oboe (287.5 Hz).

FIGURE 17: Synthesized trumpet (347 Hz).

the corresponding synthetic one, the similarity is evident and convincing.

A further refinement is to store the time envelope of the HBWT analysis coefficients and to apply it on the resynthesis coefficients.

As a consequence of these refinements the quality of the reproduced sounds improved significantly at the expense of a larger number of parameters.

7. CONCLUSIONS

In this work we introduced a new method for sound synthesis that allows us to control and reproduce the microfluctuations present in real life voiced sounds. This method is a sort of additive synthesis where one adds not only the harmonics but also modulated $1/f$ signals. We defined a new class of stochastic processes, that is, the pseudo-periodic $1/f$-like noise. We introduced a new type of multiwavelet transform useful for

the representation of these processes, the harmonic-band wavelet transform. We devised an efficient analysis/synthesis scheme able to perform parameter estimation and to generate pseudo-periodic $1/f$-like noise.

The claim of this method is that it allows to reproduce stochastic fluctuations in sounds by means of a very restricted number of parameters. Some limitations of the method are apparent when applied to real life sounds: the presence of non $1/f$ noise components due to external sources as the excitation devices requires an extension of our model.

APPENDIX A

We prove Proposition 1 of Section 4. We form

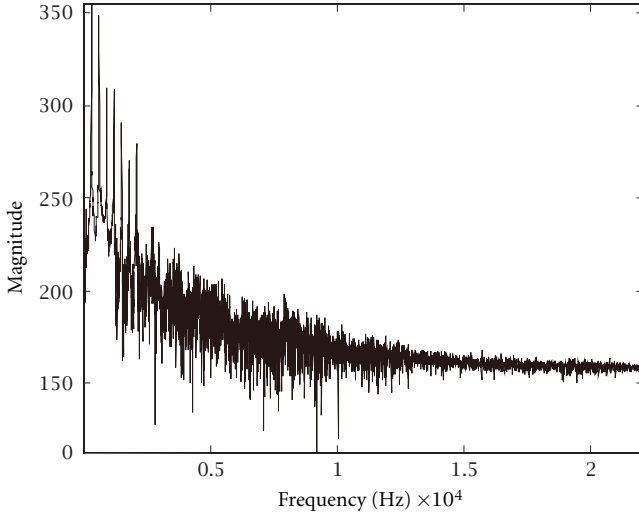$$s(t) = \sum_{q=0}^{\infty} \sum_{k=-\infty}^{\infty} v_q(k) g_{q,k}(t), \tag{A1}$$
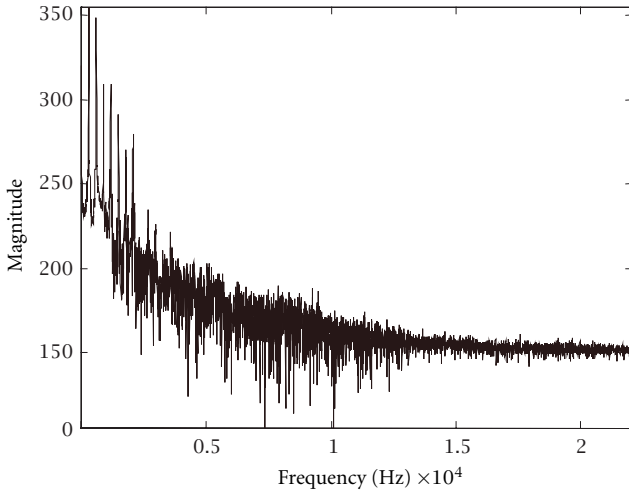
FIGURE 18: Real-life flute (298 Hz).

FIGURE 19: Synthesized flute (298 Hz).

where

$$g_{q,k}(t) = g_{q,0}(t - kT_P) \tag{A2}$$

with

$$g_{q,0}(t) = \frac{1}{\sqrt{T_P}} \cos\left(\frac{2q+1}{2T_P}\pi t\right) \operatorname{sinc}\left(\frac{t}{2T_P}\right),$$

$$v_q(k) = \frac{1}{\sqrt{T_P}}\left(\sum_{n=1}^{N}\sum_{m=-\infty}^{\infty} b_{n,q}(m)\psi_{n,m}(k) \right.$$

$$\left. + \sum_{m=-\infty}^{\infty} a_{N,q}(m)\phi_{N,m}(k)\right). \tag{A3}$$

From Lemma 2 we know that $s(t)$ is $2^N T_P$-ciclostationary.

Then the time-average power spectrum of the process $s(t)$ is

$$\bar{S}(\omega) = \int_{-\infty}^{\infty} \bar{R}_s(\tau)e^{-j\omega\tau}d\tau$$

$$= \int_{-\infty}^{\infty} \frac{d\tau}{2^N T_P}e^{-j\omega\tau}\int_{-2^N T_P/2}^{2^N T_P/2} R_s(t, t+\tau)\, dt, \tag{A4}$$

which can be written as follows:

$$\bar{S}(\omega) = \frac{1}{2^N T_P}\int_{-2^N T_P/2}^{2^N T_P/2} dt \int_{-\infty}^{\infty} d\tau$$

$$\times \sum_{q,q'=0}^{\infty}\sum_{r,r'=-\infty}^{\infty} L_{k,k';r,r'}(t,\tau)$$

$$\times R_{v_q}(k, k'+2^N(r'-r))e^{-j\omega\tau}, \tag{A5}$$

where

$$L_{k,k';r,r'}(t,\tau) = \sum_{k,k'=0}^{2^N-1} g_{q,0}(t - kT_P - 2^N rT_P)$$

$$\times g_{q',0}(t+\tau - k'T_P - 2^N r'T_P). \tag{A6}$$

The trick of the proof is to exploit the 2^N WSCS of the $v_q(m)$ proved in Lemma 1, in order to transform the finite integral over t into an integral over $(-\infty, \infty)$ equal to $G_{q,0}^*(\omega)$, that is, the complex conjugate of the Fourier transform of $g_{q,0}(t)$. After routine calculations we obtain

$$\bar{S}(\omega) = \frac{1}{2^N T_P}\sum_{q=0}^{\infty}\left|G_{q,0}(\omega)\right|^2$$

$$\times \sum_{r=-\infty}^{\infty}\sum_{k=0}^{2^N-1} R_{v_q}(k, k+r)e^{-jr\omega T_P} \tag{A7}$$

$$= \frac{1}{T_P}\sum_{q=0}^{\infty}\left|G_{q,0}(\omega)\right|^2 \bar{S}_q(\omega T_P),$$

where $\bar{S}_q(\omega T_P)$ is the time-average power spectrum of the nearly $1/f$ processes bandlimited and modulated to the band (17). The result in (6) concludes our proof.

REFERENCES

[1] M. S. Keshner, "$1/f$ noise," *Proc. IEEE*, vol. 70, no. 3, pp. 212–218, 1982.

[2] D. T. Gillespie, "The mathematics of brownian motion and johnson noise," *Amer. J. Phys.*, vol. 64, pp. 225–240, 1996.

[3] P. Flandrin, "Wavelet analysis and synthesis of fractional Brownian motion," *IEEE Trans. Inform. Theory*, vol. 38, no. 2, part 2, pp. 910–917, 1992.

[4] M. Deriche and A. H. Tewfik, "Signal modeling with filtered discrete fractional noise processes," *IEEE Trans. Signal Processing*, vol. 41, no. 9, pp. 2839–2849, 1993.

[5] G. W. Wornell, "Wavelet-based representations for the $1/f$ family of fractal processes," *Proc. IEEE*, vol. 81, no. 10, pp. 1428–1450, 1993.

[6] G. Evangelista, "Comb and multiplexed wavelet transforms and thier applications to signal processing," *IEEE Trans. Signal Processing*, vol. 42, no. 2, pp. 292–303, 1994.

[7] G. Evangelista, "Pitch synchronous wavelet representations of speech and music signals," *IEEE Trans. Signal Processing*, vol. 41, no. 12, pp. 3313–3330, 1993 special issue on Wavelets and Signal Processing.

[8] I. Daubechies, *Ten Lectures on Wavelets*, Society for Industrial and Applied Mathematics (SIAM), Philadelphia, April 1992.

[9] S. G. Mallat, "Multiresolution approximations and wavelet orthonormal bases of $L^2(\mathbf{r})$," *Trans. Amer. Math. Soc.*, vol. 315, no. 1, pp. 69–87, 1989.

[10] S. Mallat, *A Wavelet Tour of Signal Processing*, Academic Press, California, 1998.

[11] M. Vetterli and J. Kovacević, *Wavelets and Subband Coding*, Prentice Hall, 1995.

[12] P. P. Vaidyanathan, *Multirate Systems and Filter Banks*, Prentice-Hall, 1993.

[13] T. Q. Nguyen and R. D. Koilpillai, "The theory and design of arbitrary-length cosine-modulated filter banks and wavelets, satisfying perfect reconstruction," *IEEE Trans. Signal Processing*, vol. 44, no. 3, pp. 473–483, 1996.

Pietro Polotti received the laurea in physics (summa cum laude) from the University of Trieste, Trieste Italy, in 1997. In 1998 he received the diploma in Electronic Music from the Conservatorio B. Marcello, Venice, Italy. In 1999 he attended the Doctoral School of Communication System at the Polytechnic of Lausanne, Switzerland. He is now research assistant and Ph.D. student at the Communication System Department in the Audio-Visual Communication Laboratory at the Polytechnic of Lausanne, Switzerland. His interests include sound and music signal processing, multirate signal processing, wavelets, electronic music.

Gianpaolo Evangelista received the laurea in physics (summa cum laude) from the University of Napoli, Napoli, Italy, in 1984 and the M.Sc. and Ph.D. degrees in electrical engineering from the University of California, Irvine, in 1987 and 1990, respectively. Since 1998 he has been a Scientific Adjunct with the Laboratory for Audiovisual Communications, Swiss Federal Institute of Technology, Lausanne, Switzerland, on leave from the Department of Physical Sciences, University of Napoli Federico II, which he joined in 1995 as a Research Associate. From 1985 to 1986, he worked at the Centre d'Etudes de Mathématique et Acoustique Musicale (CEMAMu/CNET), Paris, France, where he contributed to the development of a DSP-based sound synthesis system, and from 1991 to 1994, he was a Research Engineer at the Microgravity Advanced Research and Support (MARS) Center, Napoli, where he was engaged in research in image processing applied to fluid motion analysis and material science. His interests include speech, music, and image processing; coding; wavelets; and multirate signal processing. Dr. Evangelista was a recipient of the Fulbright fellowship.